Analysis of Key Factors Affecting Electronic Transformer Calibration System Error

Mingzhu Zhang[1], Zhenxing Li[2]
[1]*School of Mathematics and Statistics, Xuchang University, Henan Province, China*
[2]*State Key Laboratory of Advanced Electromagnetic Engineering and Technology, Huazhong University of Science and Technology, Hubei Province, China*
zmz_xctc@126.com

***Abstract*—Recently, electronic instrument transformers (EIT) meet some problems such as high error and instability in practical application, and some new EITs and the calibration system of electronic instrument transformers (CSEIT) are attracting wide concern. In this paper, some key factors affecting CSEIT error, including sampling synchronization, digital signals processing and error estimation of the calibration system itself, are analysed, and the corresponding solutions are also offered. Sampling synchronization is realized by outputting second pulse and trigger pulse at the same time, and the length of pulses response has been controlled in a short period. Digital signal processing synthesizes some special design such as FIR digital filter, industrial frequency measurement and zero-phase filter to overcome the effects of harmonics and noise, and uses FFT interpolated algorithm based on Hanning window to eliminate the calculation error when fundamental frequency spectrum leakage happens. A novel error estimation scheme of CSEIT is proposed based on the instruments with lower measuring error. Results of the error estimation of the CSEIT itself show that the system can reach the error of 0.01 % in magnitude and 30 second in phase at rated operation state.**

***Index Terms*—Electronic instrument transformer, calibration system, interpolation algorithm, error estimation.**

I. INTRODUCTION

Electronic instrument transformers (EIT) have been greatly developed and applied in engineering for its advantages in coping with the problem of easy saturation and secondary output signals attenuation which exist in traditional electromagnetic instrument transformer [1], [2]. However, the frequent occurrence of problems such as high error and instability of EIT bring a large impact on power system protection and control in recent years [3]. And these problems have attracted more and more attention.

Digital output of EIT is the main reason to change the conventional transformer calibration system [4]. At present, a lot of engineers utilize high-accuracy acquisition cards or instruments to acquire secondary output signals of EIT [5]–[7]. Reference [5] proposes the earliest calibration system of electronic instrument transformers (CSEIT) on virtual instrument platform based on acquisition PCI 6013 card (produced by NI Company). But the error of CSEIT is big for using the card with the error of 0.03 %. Reference [6] designs special digital sampling system as the sampling system of reference source signal, which estimated relative uncertainty is within 4.0×10-7 in magnitude and within 40 μrad in phase. But the error estimation of CSEIT is lack of certain feasibility for the system design is based on the comparisons of the two same measurement systems. Reference [7] utilizes PCI card based on a high-accuracy analogue-to-digital (A/D) converter with the error of 0.01 % as digital sampling system of CSEIT, whose error exceeds 0.03 % in magnitude error and 1 min in phase error. But the calibration results change greatly under the condition of power frequency fluctuations.

Although some papers have described the overall designs of CSEIT, it is still lack of systematic discussions for some key technologies, especially for digital signal processing and the error estimation of CSEIT itself [8], [9]. In this paper, some key factors affecting CSEIT error, including sampling synchronization, digital signals processing and the error estimation of the system itself, are analysed, and the corresponding solutions are also offered for the purpose of designing a CSEIT with the error of 0.01 % which can calibrate the EITs with the error of 0.2 %.

II. PRINCIPLE OF CSEIT

A CSEIT mainly consists of three aspects: transformation of high-voltage reference signal, synchronous sampling and communication of digital signal, and comparison between reference signal and tested EIT signal. Taken the CSEIT for electronic current transformer for example, the basic principle is shown in Fig. 1.

In Fig. 1, the current booster transforms AC 380 V into current source with range of 1.2 times rated current of tested EIT. The electronic current transformer (ECT) and merging unit constitute the tested instrument system together. The reference current transformer, digital sampling system (DSS), synchronization system and operation platform constitute the calibration system together.

Manuscript received May 8, 2012; accepted January 16, 2013.
This research was funded by a grant (No. 12A110022) from Henan Province Department of Education Natural Science Foundation of China, and a grant (No. 122300410269) from the Henan Province Science and Technology Department Natural Science Foundation of China.

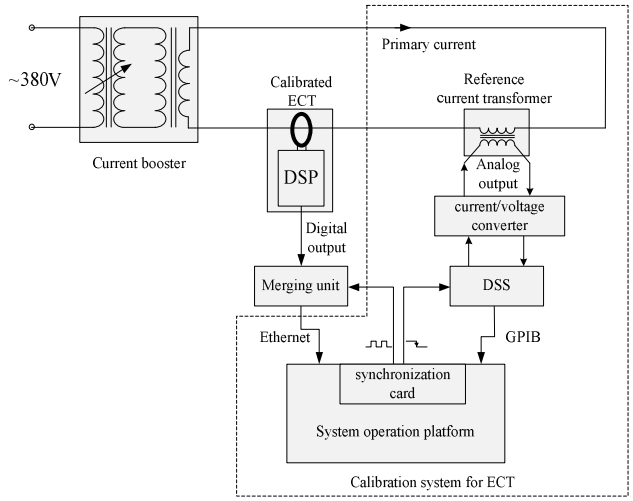

Fig. 1. Schematic diagram of calibration system for electronic current transformer.

III. KEY FACTORS AFFECTING CSEIT ERROR

A. Selection of reference instrument transformer

At present, the function of CSEIT is mainly based on the comparison of two channels of signals, and the emphasis of some studies is centralized on the processing of the secondary output signal. In fact, the error of the transformation for high-voltage signal also affects the error of CSEIT directly. Although the electromagnetic current/voltage transformer has problems of easy magnetic saturation, big size and high cost, it has high accuracy class (0.01 % level or higher) and good stability under steady state. Hence, the electromagnetic current/voltage transformer is adopted in this paper to implement signal transformation of reference source.

B. Reference signal sampling system

High-accuracy DSS is the key to ensure the rationality of CSEIT design. Lots of papers show that the error of their CSEITs can below 0.01 % in magnitude, but the error of sampling system is higher than 0.01 %. It is obvious that the error estimation of CSEIT is not enough. The paper recommends some high-accuracy acquisition cards or instruments to design CSEIT for their stability, such as HP3458A meter with sampling precision higher than 0.01 % and the input bandwidth as large as 150 kHz [10].

C. Sampling synchronization

Sampling synchronization of digital signals is critical for CSEIT. The synchronization error is the key to affect the error of CSEIT, especially in condition that the CSEIT has different synchronization manner of the two channel signals. The sampling synchronization technology that merging unit receives second pulse and DSS receives trigger pulse is introduced for example. The schematic is shown in Fig. 2.

1) Second pulse and trigger pulse must be synchronized in trigger pulse response. As shown in Fig. 2, CSEIT will choose the first second pulse rise time after its start-up to trigger a low pulse to establish synchronization system.

2) The length of pulse response must be within the narrow range. From the Fig. 2, the length for two pulses is within 10 ns and the calibration error of CSEIT for phase is lower than 7 microseconds.

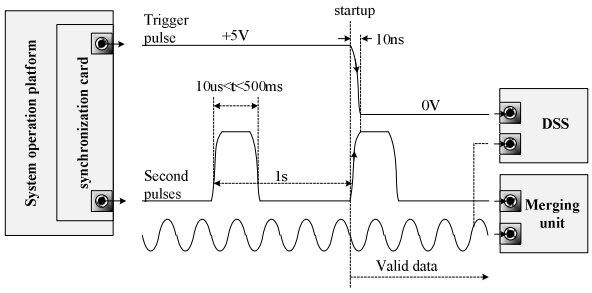

Fig. 2. Schematic diagram of sampling synchronization.

D. Digital signal processing

Besides the fundamental wave， the input signals of the reference source contain higher harmonic components and white noise especially when the amplitudes of the input signals are low, the S/N ratio decreases remarkably and the signals received by DSS contain strong interference [11]. Digital signal processing should vitally been taken into consideration. Considering that not only the amplitude but also the phase of the signals are compared in CSEIT, the phase shift of the filter should be taken into account as well. The overall signal processing scheme is shown in Fig. 3.

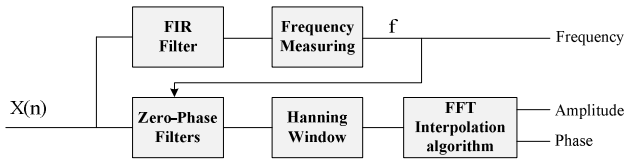

Fig. 3. Synchronization Schematic diagram of digital signal progressing.

1) FIR filter

It is aimed to remove the impact of harmonic and noise for fundamental frequency signals extraction. Given that only frequency parameter of the output signals needs to be obtained, linear phase shift and signal attenuation of the filter are not taken into account for frequency computing. Hence, FIR filter is best under high sampling frequency. The order and the bandwidth of FIR filter may be selected reasonably to get better filtering results because the CSEIT only cares about power frequency signal. It is recommended to set cut-off frequency to 75 Hz and select filter order to 45.

2) Fundamental frequency measurement

The filtered waveform is basically sine wave. The frequency can be obtained by measuring the time interval between two adjacent zero crossing points. But the value of the sampling points is not just equal to zero. The time of zero crossing can be gotten by fitting curve on the two discrete sampling points which are before and behind the zero crossing point respectively. The measuring principle is shown in Fig. 4.

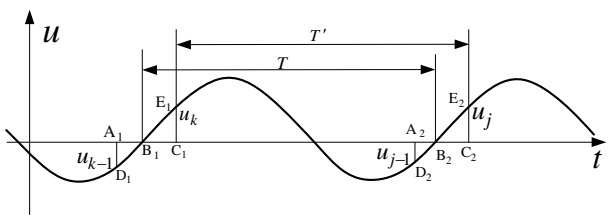

Fig. 4. The principle of frequency measurement.

From the waveform in Fig. 4, the corresponding phase angles of sampling points u_{k-1}, u_k, u_{j-1} and u_j are small under high sampling frequency, and the sine waveform between D_1E_1 can be approximately fitted by straight line $D_1B_1E_1$. Likewise, the sine waveform between D_2E_2 can be approximately fitted by straight line $D_2B_2E_2$.

Based on similar triangle theorem, we can get

$$\frac{t_{B1C1}}{t_{A1B1}} = \frac{|u_k|}{|u_{k-1}|} \Rightarrow \frac{t_{B1C1}}{t_{A1C1}}, \\ = \frac{|u_k|}{|u_{k-1}|+|u_k|} = \frac{|u_k|}{u_k - u_{k-1}}. \quad (1)$$

Setting sampling period as T_S, t_{B1C1} can be written as

$$t_{B1C1} = \frac{|u_k|}{u_k - u_{k-1}} \cdot t_{A1C1} = \frac{|u_k|}{u_k - u_{k-1}} \cdot T_S. \quad (2)$$

Similarly

$$t_{B2C2} = \frac{|u_j|}{u_j - u_{j-1}} \cdot T_S. \quad (3)$$

Then

$$t_{B1B2} = (j-k) \cdot T_S + t_{B1C1} - t_{B2C2}. \quad (4)$$

So, the tested frequency can be calculated as

$$f = \frac{1}{t_{B1B2}} = \frac{1}{(j-k) \cdot T_S + t_{B1C1} - t_{B2C2}}. \quad (5)$$

Based on the above analyses, the increase of the sampling frequency is helpful to decrease the error of frequency measurement. Furthermore, the mean value of multiple frequency measurement values is obtained to decrease calculation error.

3) Zero-Phase filter

Design of the Zero-Phase Filter, which has no phase shift for the fundamental wave signals, is of great significance to avoid the adverse impact of phase shift on phase error of calibration system. The principle shown in Fig. 5 is adopted. It contains two identical IIR filters and two deserialization units which reverse the time sequence. For any frequency component of x (n), if it has a phase angle of α and the first IIR filter causes a phase shift of $-\beta$, the phase angle of signal at node A is $\alpha - \beta$. Deserialization brings about a complex conjugate of phase angle and an additional phase shift of $-\theta$. Thus the phase angle at node B is $(-\alpha + \beta - \theta)$. The second IIR filter is the same as the first one, so phase angle at node C is $(-\alpha - \theta)$. According to second deserialization, phase angle at node D is exactly α, which has no phase shift comparing with x (n). This zero phase shift characteristic remains valid in the whole frequency range, which is the reason why Zero-Phase Filter is named.

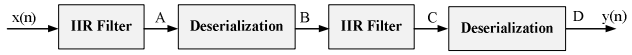

Fig. 5. Principle of zero phase shift filter.

The filtered signals, compared with the original signals, are influenced by the amplitude attenuation and phase shift. The design principle of zero phase shift filter can avoid the influence of the phase shift, but the influence of the amplitude attenuation must be solved by a compensation coefficient in design of IIR filter. The coefficient can be easily calculated based on the real time measurement frequency.

4) FFT interpolation algorithm

Apparently, power system frequency cannot remain constant. It is difficult for signal acquisition systems to maintain synchronized sampling when frequency fluctuates. When signal sampling is synchronous, DFT frequency spectrum at each point coincides with spectrum of the original signal, as shown in Figure 6(a). Meanwhile, they are not coincident when signal sampling is asynchronous, as shown in Figure 6(b), where spectrum leakage obviously exists. Window spectrum side lobe energy is smaller when signals acquisition using Hanning windows, the spectrum leakage brought by convolution is less, and the measurement error would be lower [12].

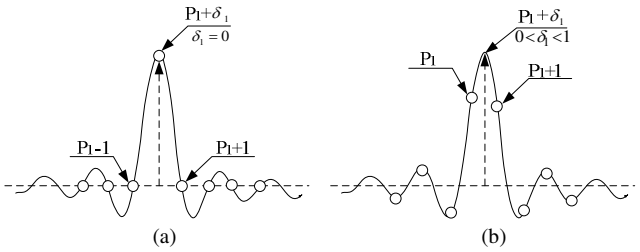

Fig. 6. Single frequency signal's spectrum: (a) synchronous sampling; (b) asynchronous sampling.

From Fig. 6, (b), the fundamental frequency f_1 corresponds with digital frequency $(P_1 + \delta_1) \cdot 2\pi / N$ when the frequency fluctuates. In Fig. 6 (b) P_1 is positive integer, N is the number of sample points in a period, and $0 \le \delta_1 < 1$. FFT interpolation algorithm is introduced as follows.

Supposing original input signal is

$$x_1(n) = A_1 e^{j(2\pi f_1 n + \varphi_1)}, n = 0,1,2 \cdots N\text{-}1. \quad (6)$$

The Hanning window function is

$$w_H(n) = (0.5 - 0.5\cos(\frac{2\pi n}{N-1})). \quad (7)$$

The original signal $X_1(K)$ in frequency domain can be calculated by DFT

$$X_1(K) = \mathrm{DFT}[x_1(n)] = \sum_{n=0}^{N-1} A_1 e^{j(2\pi f_1 n + \varphi_1)} e^{-j\frac{2\pi kn}{N}} = \\ = A_1 e^{j\varphi_1} \frac{\sin[(k - p_1 - \delta_1)\pi]}{N \sin[\frac{(k - p_1 - \delta_1)\pi}{N}]} e^{-j(k-p_1-\delta_1)\frac{(N-1)\pi}{N}}. \quad (8)$$

The signal $X_H(K)$ after Hanning windowing can be calculated by DFT

$$X_H(K) = DFT[x_1(n)w_H(n)] =$$
$$= DFT[x_1(n)(0.5-0.5\cos(\frac{2\pi n}{N-1}))] \approx$$
$$\approx DFT[x_1(n)(0.5-0.5\cos(\frac{2\pi n}{N}))] =$$
$$= DFT\{[0.5[x_1(n)-x_1(n)(\frac{e^{j\frac{2\pi n}{N}}+e^{-j\frac{2\pi n}{N}}}{2})\}] =$$
$$= 0.5\{X_1(k)-0.5[X_1(K+1)+X_1(K-1)]\}. \quad (9)$$

Substituting (8) to (9), the following expression can be obtained)

$$X_H(K) = \{\frac{\sin[(K-P_1-\delta_1)\pi]}{N\sin[\frac{(K-P_1-\delta_1)\pi}{N}]}e^{-j(K-P_1-\delta_1)\pi\frac{N-1}{N}} -$$
$$-0.5[\frac{\sin[(K-P_1-\delta_1+1)\pi]}{N\sin[\frac{(K-P_1-\delta_1+1)\pi}{N}]}e^{-j(K-P_1-\delta_1+1)\pi\frac{N-1}{N}} +$$
$$+\frac{\sin[(K-P_1-\delta_1-1)\pi]}{N\sin[\frac{(K-P_1-\delta_1-1)\pi}{N}]}e^{-j(K-P_1-\delta_1-1)\pi\frac{N-1}{N}}]\}0.5A_1e^{j\varphi_1}. \quad (10)$$

Approximate equation, $\sin(\frac{\theta}{N}) \approx \theta$, $e^{\pm j\frac{(N-1)\pi}{N}} \approx -1$, can be used when N>>1. And the frequency spectrum $X_H(P_1)$ of P_1 point can be calculated based on the (10) when $K = P_1$.

$$X_H(P_1) = \frac{1}{2}A_1e^{j\varphi_1}\{\frac{\sin(\delta_1\pi)}{\delta_1\pi}e^{j\frac{(N-1)\delta_1}{N}\pi} -$$
$$-\frac{1}{2}[\frac{\sin(\delta_1\pi)}{(\delta_1-1)\pi}e^{j\frac{(N-1)\delta_1}{N}\pi}+\frac{\sin(\delta_1\pi)}{(\delta_1+1)\pi}e^{j\frac{(N-1)\delta_1}{N}\pi}]\} =$$
$$= \frac{A_1\sin(\delta_1\pi)}{2\delta_1(1-\delta_1^2)\pi}e^{j\varphi_1+\frac{(N-1)\delta_1}{N}\pi}. \quad (11)$$

Similarly, the frequency spectrum $X_H(P_1+1)$ of (P_1+1) point can be obtained when $K = P_1+1$

$$X_H(P_1+1) = \frac{A_1\sin(\delta_1\pi)e^{j\varphi_1+\delta_1\pi}}{2\delta_1(1-\delta_1)(2-\delta_1)\pi} \quad (12)$$

Let

$$\beta_1 = \frac{|X_H(P_1)|}{|X_H(P_1+1)|} = \frac{\frac{A_1\sin(\pi\delta_1)}{2\pi\delta_1(1-\delta_1^2)}}{\frac{A_1\sin(\pi\delta_1)}{2\pi\delta_1(1-\delta_1^2)(2-\delta_1)}} \quad (13)$$

Hence

$$\delta_1 = \frac{2\beta_1-1}{1+\beta_1}. \quad (14)$$

According to (11) and (14), the values of industrial frequency signal amplitude and phase angle with high precision can be obtained as:

$$A_1 = |X_H(P_1)|\cdot\frac{[2\pi\delta_1(1-\delta_1^2)]}{\sin(\pi\delta_1)}, \quad (15)$$

$$\varphi_1 = angle(X_H(P_1)) - \frac{(N-1)\delta_1}{N}\pi. \quad (16)$$

IV. Error Estimation of CSEIT

The error estimation of the designed CSEIT itself is a very important part in the design process of the calibration system. In this paper, the measuring instruments with higher precision are used for the error estimation of the designed CSEIT.

A. Error estimation of magnitude

Error estimation of the magnitude is essential to verify the calculated RMS value of the reference signals. The schematic diagram is shown in Fig. 7. Reference [13] concludes that FLUKE 5720A has a precision of five per ten thousand when the output voltage is within the range of 2 mV to 220 mV, while the precision is not lower than one per ten thousand when the output is over 220 mV. Taking output voltage U_N of FLUKE 5720A as reference and RMS value calculated in CSEIT U as test subject, the magnitude error of CSEIT is defined as

$$e_{rms} = \frac{U-U_N}{U_N}\times 100\%. \quad (17)$$

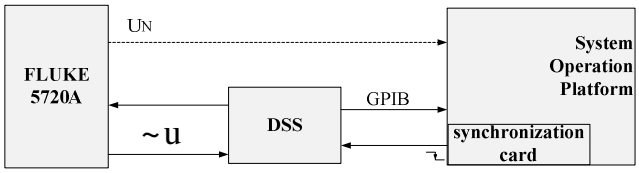

Fig. 7. Schematic diagram of error estimation for magnitude.

Considering the impact of frequency error and asynchronous sampling, the maximum, minimum and mean statistical error among 100 tests of the error estimation under different frequency (49 Hz, 50 Hz and 51 Hz) and different output voltage of Fluke 5720A (5 mV, 50 mV, 1 V and 57.7 V) are listed in Table I.

TABLE I. TEST RESULTS OF ERROR ESTIMATION OF MAGNITUDE.

Results (e_{rms})		Max. (%)	Min. (%)	Mean (%)
49Hz	5 mV	0.071	-0.002	0,052
	50 mV	0.052	-0.030	0.025
	1 V	0.035	0.014	0.011
	57.7 V	0.015	-0.006	0.009
50Hz	5 mV	0.043	-0.085	0,002
	50 mV	0.002	-0.010	-0.000
	1 V	0.005	0.004	0.004
	57.7 V	0.005	-0.006	-0.005

Results (e_{rms})		Max. (%)	Min. (%)	Mean (%)
51Hz	5 mV	0.043	-0.085	-0.061
	50 mV	0.022	-0.056	-0.042
	1 V	0.015	-0.034	-0.023
	57.7 V	0.003	-0.026	-0.012

The results of error estimation of magnitude indicate that the error of CSEIT reaches level of 0.01 % in magnitude under basic frequency and has little restriction on frequency fluctuations.

B. Error estimation of phase

Error estimation of phase is essential to verify the time delay of EIT signal. The schematic diagram is shown in Fig. 8. BHE-I, Phase-modulation instrument, which provides a phase error lower than 1'', outputs two identical signals with a phase shift of $\Delta\varphi$ between them. One is captured by oscilloscope TEK MSO3034 with high sampling rate. The captured phase of the oscilloscope, φ_1, is delivered to calibration system. The other is captured by digital sampling system. The phase φ_2 is calculated in CSEIT. Taking $\Delta\varphi$ as reference and $\varphi_1 - \varphi_2$ as test subject, the phase error of CSEIT is defined as

$$e_{\varphi} = (\varphi_1 - \varphi_2) - \Delta\varphi . \quad (18)$$

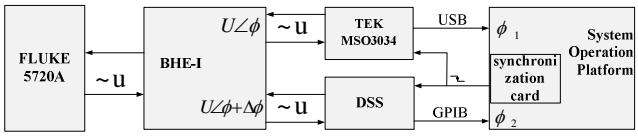

Fig. 8. Schematic diagram of error estimation for phase.

Considering the impact of frequency offset and asynchronous sampling, the maximum, minimum and mean statistical error among 100 tests of the error estimation under different frequency (49 Hz, 50 Hz and 51 Hz) and different output $\Delta\varphi$ of BHE (0, 2'12", 5'33" and 16'39") are listed in Table II.

TABLE II. TEST RESULTS OF ERROR ESTIMATION OF PHASE.

Results (e_{φ})		Max.	Min.	Mean
49Hz	0	0'7"	0'1"	0'5"
	2'12"	0'6"	-0'3"	0'3"
	5'33"	0'10"	-0'4"	0'6"
	16'39"	0'28"	-0'35"	-0'15"
50Hz	0	0'6"	-0'2"	0'4"
	2'12"	0'2"	-0'1"	0'2"
	5'33"	0'5"	-0'3"	0'2"
	16'39"	0'25"	-0'18"	0'14"
51Hz	0	0'1"	-0'4"	-0'3"
	2'12"	0'1"	-0'6"	-0'4"
	5'33"	0'4"	-0'12"	-0'10"
	16'39"	-0'8"	-0'38"	-0'25"

The results of error estimation of phase indicate that the error of CSEIT is no more than 30 second in phase error under basic frequency and has little restriction on frequency fluctuations.

V. FIELD TESTS

The entire calibration system designed by this paper is applied in field tests of electronic current transformer (ECT) and electronic voltage transformer (EVT) in Sanxiang smart substation located in Guangdong, China. The main test results are listed here.

A. Calibration of ECT

An ECT with the error of 0.2 % is calibrated according to the principle in Figure 1. Rated primary current of the ECT is 300A; inherent delay is 188μs. Each test under different input signal is tested for 10 times. The statistical results are listed in Table III.

TABLE III. TEST RESULTS OF A-PHASE CURRENT.

Inputs		Max.	Min.	Mean
5 % (In)	Mag. Error	-0.288 %	-0.306 %	-0.297 %
	Ph. Error	6′24″	4′41″	5′20″
10 % (In)	Mag. Error	-0.167 %	-0.182 %	-0.176 %
	Ph. Error	1′27″	1′02″	1′11″
30 % (In)	Mag. Error	-0.143 %	-0.155 %	-0.151 %
	Ph. Error	1′44″	0′42″	1′21″
50 % (In)	Mag. Error	-0.120 %	-0.128 %	-0.124 %
	Ph. Error	0′47″	0′32″	0′42″
80 % (In)	Mag. Error	-0.108 %	-0.118 %	-0.112 %
	Ph. Error	1′18″	1′01″	1′14″
100 % (In)	Mag. Error	-0.101 %	-0.112 %	-0.105 %
	Ph. Error	1′35″	1′15″	1′26″

The results indicate that the magnitude error of the ECT is less than 0.2 % and the phase error is less than 2 second when the input current equals to rated value; and the magnitude error of the ECT is less than 0.5 % and the phase error is less than 10 second when the input current unequal to rated value. Based on the test results and IEC 60044-8 standard, the error of the tested ECT reaches the class of 0.2 %.

B. Calibration of EVT

An EVT with the error of 0.2 % is calibrated according to the principle in Figure 1. Rated primary voltage of the EVT is 110kV; inherent delay is 255μs. Each test under different input signal is tested for 10 times. The statistical results are listed in Table IV.

TABLE IV. TEST RESULTS OF A-PHASE VOLTAGE.

Inputs		Max.	Min.	Mean
70 %（Vn）	Mag. Error	0.150 %	0.130 %	0.141 %
	Ph. Error	6′21″	4′66″	5′21″
80 %（Vn）	Mag. Error	0.129 %	0.118 %	0.125 %
	Ph. Error	3′69″	3′74″	3′66″
100 %（Vn）	Mag. Error	0.075 %	0.064 %	0.068 %
	Ph. Error	0′45″	0′31″	0′37″
110 %（Vn）	Mag. Error	0.178 %	0.097 %	0.153 %
	Ph. Error	2′50″	1′10″	1′57″

The results indicate that the magnitude error of the EVT is less than 0.2 % and the phase error is less than 2 second when the input voltage equals to rated value; and the magnitude error of the EVT is less than 0.2 % and the phase error is less than 10 second when the input voltage unequal to rated value. Based on the test results and IEC 60044-7 standard, the error of the tested EVT reaches the class of 0.2 %.

VI. CONCLUSIONS

To decrease the error of the calibration system of electrical instrument transformer, a comprehensive digital signal processing method is proposed based on digital filter and FFT interpolation algorithm. At the same time, the other key factors affecting CSEIT error, including selection of reference instrument transformer, reference signal sampling system, and sampling synchronization are also discussed in this paper. The results of error estimation of CSEIT show the error of the calibration system based on the proposed method reaches level of 0.01 % in magnitude and is not more than 30 second in phase at rated operation state. The entire calibration system is also applied in field tests. The results of field tests show that the implemented calibration system was successfully applied in field to calibrate ECT and EVT both with the error of 0.2 %.

REFERENCES

[1] J. D. Ramboz, "Machinable Rogowski coil, design, and calibration", *IEEE Transaction on instrumentation and measurement*, vol. 45, no. 2, pp. 511–515, 2002. [Online]. Available: http://dx.doi.org/10.1109/19.492777

[2] Huiqing Pan, Shulin Tian, "An Adaptive Synthesis Calibration Method for Time interleaved Sampling Systems", *Metrology and Measurement System*, vol. 3, no. 3, pp. 405–414, 2010.

[3] Ding Tao, Xu Erqiang, "Measurement and Problem's Analysis of the On–site Error for Electronic Transformer", *Electrical Measurement & Instrumentation*, vol. 48, no. 3, pp. 36–39, 2011.

[4] E. P. Suomalainen, J. K. Hällström, "Onsite Calibration of a Current Transformer Using a Rogowski Coil", *IEEE Transactions on Instrumentation and Measurement*, vol. 58. no. 4, pp. 1054–1058, 2009. [Online]. Available: http://dx.doi.org/10.1109/TIM.2008.2007031

[5] Mei Zhi Gang, Luo Cheng Mu, "Design of Virtual Calibrator for Instrument Transformer", *Transforme,* vol. 43, no. 5, pp. 25–29, 2006.

[6] B. Djokic, E. So, "Calibration System for Electronic Instrument Transformers with Digital Output", *IEEE Transaction on instrumentation and measurement*, vol. 54, no. 2, pp. 479–482, 2005. [Online]. Available: http://dx.doi.org/10.1109/TIM.2004.843420

[7] F. Pan, Y. Xu, "Calibration System for Electronic Instrument Transformers with Analogue and Digital Outputs", in *Proc. of the 9th International Conference on Electronic Measurement & Instruments*, vol. 1, 2009, pp. 650–654.

[8] Tian Qi Xu, Xiang Gen Yin, "Analysis on functionality and feasible structure of wide area protection system", *Power System Protection and Control,* vol. 38, no. 3, pp. 93–97, 2009.

[9] M. Gurbiel, P. Komarnicki, "Merging unit accuracy testing", in *Proc. of the IEEE Power & Energy Society General Meeting*, 2009, pp.1–6.

[10] A. Brandolini, M. Faifer, "A Simple Method for the Calibration of Traditional and Electronic Measurement Current and Voltage Transformers", *IEEE Transaction on Instrumentation and Measurement*, vol. 58, no. 5, pp. 1345–1353, 2009. [Online]. Available: http://dx.doi.org/10.1109/TIM.2008.2009184

[11] *Agilent 3458A Multimeter, User manual*. [Online]. Available: http://www.home.agilent.com/agilent/facet.jspx?cc=CN&lc=chi&k=3458A&sm=g. 2000

[12] F. Li, H. Wang, "Realization of high precision harmonics analysis with pleisiochronous DFT arithmetic", *J Tsinghua University*. vol. 39, pp. 47–50, 1999.

[13] P. Bilski, W. Winiecki, "Virtual Spectrum Analyzer Based on Data Acquisition Card", *IEEE Transaction on Instrumentation and Measurement*, vol. 51, no. 1, pp. 82–87, 2002. [Online]. Available: http://dx.doi.org/10.1109/19.989906

[14] *FLUKE 5720A Multi–Function Calibrator, User manual.* [Online]. Available: http://www.fluke.com.cn/fluke/htmlDocument/2010-12-16/ detail_1390.html.1996